Advances in Science and Technology Research Journal

Advances in Science and Technology Research Journal 2023, 17(2), 12–24
https://doi.org/10.12913/22998624/158838
ISSN 2299–8624, License CC-BY 4.0

Received: 2022.12.29
Accepted: 2023.03.01
Published: 2023.04.01

Analysis of Torsional Strength of Pa2200 Material Shape Additively with the Selective Laser Sintering Technology

Jacek Bernaczek[1*], Mariusz Dębski[1], Małgorzata Gontarz[1], Roman Grygoruk[2], Jerzy Józwik[3], Bogdan Kozik[1], Piotr Mikulski[4]

[1] The Faculty of Mechanical Engineering and Aeronautics, Department of Mechanical Engineering; Rzeszow University of Technology, Aleja Powstańców Warszawy 12, 35-959 Rzeszów, Poland

[2] Institute of Mechanics and Printing, Department of Machine Design and Biomedical Engineering, Warsaw University of Technology, plac Politechniki 1, 00-661 Warszawa, Poland

[3] Faculty of Mechanical Engineering, Department of Production Engineering, Lublin University of Technology, ul. Nadbystrzycka 38 D 20 – 618 Lublin, Poland

[4] BIBUS MENOS Sp. z o.o.; ul. Spadochroniarzy 18, 80-298 Gdańsk, Poland

* Corresponding author's e-mail: jbernacz@prz.edu.pl

ABSTRACT

The purpose of the undertaken research work is to analyze the torsional strength of standard samples with a circular cross-section, produced additively using the Selective Laser Sintering (SLS) technique – sintering PA2200 polyamide powders. The studies conducted so far have not included a static torsion test, the results of which are crucial for parts such as machine shafts, hubs, couplings, etc. Hence the idea of conducting the research in question. The samples were made in different settings relative to the machine's working platform and subjected to post-processing in two variants – by water-soaking and furnace-heating – in order to determine the influence of the orientation of the model in the manufacturing process and the type of post-processing on torsional strength. The produced samples were additionally subjected to a preliminary dimensional and shape verification due to the significant impact of the accuracy of the models in the SLS process on the operation of the above-mentioned machine parts. Based on the analysis of the test results, it was found that the highest torsional strength was determined for the furnace-heated samples. In addition, the highest mapping accuracy was found for models positioned vertically in relation to the machine's working platform.

Keywords: torsional strength, PA2200 powder, additive manufacturing, SLS technology, optical measurements, 3D scanning.

INTRODUCTION

The field of applications of additively manufactured parts is currently very wide and includes various industries mostly, medicine, aerospace, architecture, etc. [1, 2, 3]. Elements shaped with additive manufacturing techniques are used not only in the process of physical verification and preliminary tests at the designand implementation stage of new products [4, 5]. They are also increasingly used as final parts [6, 7]. The reason for this situation is the dynamic development of AM (Additive Manufacturing) technologies. New manufacturing solutions are developed, key techniques of layered material processing are modified and improved [8], and above all, the range of available model materials is expanded [9]. However, the possibility of using a given method in a specific area of application is conditioned primarily by the parameters of the materials and the accuracy of the dimensional and shape mapping of the models in the process in question [10, 11, 12]. The data declared by the manufacturers in the vast majority differ from the

actual results determined by laboratory tests. The reason for such discrepancies are the individual conditions of the elementary AM process, which includes things like: the operating conditions of the machine, user-defined process parameters [13], development of CAD/STL/RP (Computer Aided Design / Standard Triangulation Language / Rapid Prototyping) numerical data or the type of final processing and post-processing adequate for the selected technique, material type and the application spectrum of built part [14, 15]. Additionally, torsional strength parameters are not provided which based on the possibilities provided by additive manufacturing of wide variety of parts loaded with a torsion moment, are extremely important in the process of their design [16, 17, 18]. Some of the additively manufactured parts are shafts, couplings, gear hubs, for which one of the key parameters is torsional strength [19]. In addition, the values of dimensional and shape deviations are extremely important in this case – circularity deviation, cylindricity deviation, coaxiality of the model with the CAD nominal cylinder, total runout. Therefore, further research work is necessary to determine reliable – real values of the above-mentioned parameters for commonly used AM methods and model materials [20, 21].

In this study an SLS process was performed on EOS Formiga P100 machine with layer thickness of 0.1 mm and manufacturer exposition process –„PA2200 Performance 1.0". Laser energy density used in this process was 0.067 J/mm^2 with laser power set at 25 W and hetch lines laser scanning speed of 1500 mm/s, with laser scanning line distance of 0.25 mm [22]. The laser focus spot diameter was set to 0.42 mm.

PA2200 in its pre sintered form is a white powder that is mainly pure PA12 polymer (12-aminododecanoic acid lactam) with additive of proprietary heat and oxidation stabilizers (one of which is titanium dioxide). Powder granedie meter is between 0.03 – 0.120 mm and is highly spherical with distorted„potato – like" shaped granes. Typical sintered material is a 50/50% mixture of used, sieved powder from earlier sintering process with fresh powder. This procedure is used to prevent the powder from influence of thermal degradation that occurs during sinterization process. Constant powder refreshment is a key factor for constant mechanical properties and dimensional accuracy of built elements throughout the production process [22, 23, 24]. PA2200 powder is certified biocompatible material according to EN ISO 109993–1 and USP / level VI / 121 °C and due to its properties and quality is also widely used in medica industry for surgical guides and tooling.

The SLS process used in this research served for manufacturing of standard circular samples [25]. Individual model groups were arranged in three orientations relative to the build platform of the machine – vertically, horizontally and at an angle of 45°. Two sets of samples were prepared for final processing by water-soaking and furnace-heating. The first stage of the research was the verification of the dimensions and shape of the samples by optical measurements using an advanced 3D scanner system. Then, the samples were subjected to additional treatment in the two post-processing variants indicated above, i.e. soaking and heating. Torsional strength tests were carried out using a proprietary torsion loads test apparatur equipped with an advanced measurements system for determining the torsional moment and torsion angle, as well as a precise adjustable drive system. The last stage of research work was the analysis of sample fracture.

The analysis of scientific studies in the area of SLS technology for polymer powders shows the lack of publication of data on torsional strength. A number of tests were carried out to determine other material properties, taking into account the impact of the parameters of the SLS manufacturing process on individual strength parameters [26, 27, 28]. Therefore, it was important to undertake the research, the results of which will complement the current state of knowledge and help determine the potential area of application of parts manufactured with the SLS technique from the PA2200 material.

MATERIALS AND METHODS

The model material in the form of PA2200 polymer powder was used in the research process. A list of selected, sintered PA2200 properties declared by the manufacturer is presented in Table 1.

Samples were made of the PA2200 powder on EOS Formiga P100 SLS system [29]. Mechanical properties offered by this technology and material fulfill the expectations for end use products comparable to classical processes like injection molding. Digital data for SLS process were prepared with the use of dedicated software tools that enable the placement of models in machine build

Table 1. Selected material data – based on EOS PA2200 catalog data

Property of sintered material	Value	Unit	Test standard
Tensile modulus			
X Direction Y Direction Z Direction	1700 1700 1700	MPa MPa MPa	ISO 527–1/-2
Tensile strength			
X Direction Y Direction Z Direction	50 50 50	MPa MPa MPa	ISO 527–1/-2
Strain at break			
X Direction Y Direction Z Direction	20 20 10	% % %	ISO 527–1/-2
Charpy impact strength (+23 °C, X direction)	53	kJ/m^2	ISO 527–1/-2
Charpy notched impact strength (+23 °C, X direction)	4.8	kJ/m^2	ISO 527–1/-2
Flexural modulus (23 °C, X direction)	1500	MPa	ISO 178
Izod impact notched (23 °C X direction)	4.4	kJ/m^2	ISO 180/1A
Shore D hardness (15s)	75	-	ISO 7619–1
Density (laser sintered)	930	kg/m^3	EOS method
Thermal properties			
Melting temperature (20 °C/min)	176	°C	ISO 11357–1/-3
Vicat softening temperature (50 °C/h 50N)	163	°C	ISO 306

space, layer preparation and information for laser exposition. The arrangement of the samples in the build space is shown in Figure 1.

SLS process does not require any support structures as unsintered powder is sufficient for holding sintered layers in place. One of the major limitations to SLS process that needs to be taken under consideration regarding parts mechanical properties is minimal wall thickness. Walls bellow 3 mm thickness will show large difference in mechanical properties in comparison to thicker walls as the parts are more porous closer to their surface then in their core. The above-mentioned problem is visible when the same structures are produced in different positions in the working space [30]. This phenomenon is caused by difference of energy density and heat influence on connection of layer contour exposition and core exposition.

Figure 2 shows SLS samples produced for the purpose of the research procedure in question. Two series of models of 12 pieces were produced – 4 samples each for 3 orientations of the model in the working space (Fig. 1). There were 4 samples built in vertical orientation to layer growth (along Z axis in SLS machine), 4 samples in 45° orientation to XY plane and 4 samples built along X orientation.

The first stage of the research work in question included the process of optical measurements using a 3D scanner. The GOM Atos apparatus was used for the analysis due to its purpose for very complex measurement tasks and the guarantee of extremely precise measurements for small

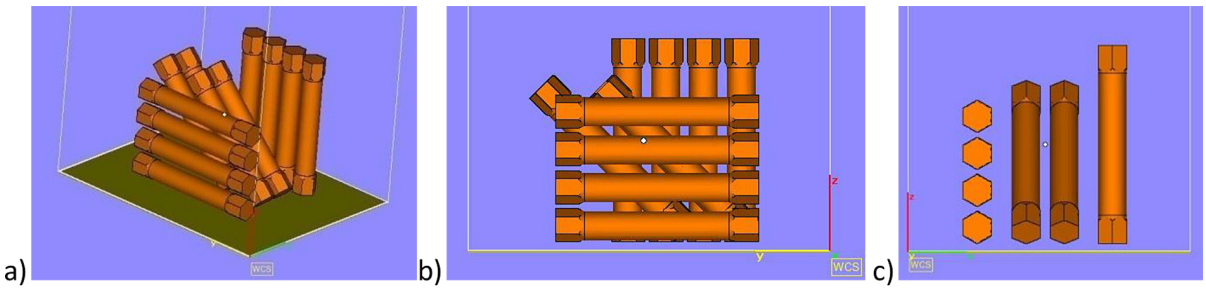

Figure 1. Arrangement of samples in the working space: a) isometric view, b) front view, c) side view

Figure 2. SLS samples

and medium-sized parts. The scanner uses blue light technology in a narrow band, which enables effective filtration of light noise from the environment. Structural light in the form of stripes is projected onto the tested object from a centrally placed projector. Advanced cameras are installed on both sides of the projector to record the deflection of the projected light fringes within the geometric changes of the measured part. Spatial digitalization with a 3D scanner allows to observe the path of technological lines of creation of individual layers of material. this allows an initial visual assessment of the quality of the model and the creation of the target accuracy in selected areas of the model. these lines in the nomenclature of 3D printing are called step effect.

The next stage of the research procedure was the preparation of samples in two variants of final treatment – by water-soaking and furnace-heating. According to manufacturer recommendations sintered parts can be enhanced by humidification as PA12 increases its ductility after reaching its maximum water absorption in its structure [31]. Effect of humidification of sintered part should have influence on mechanical properties especially part ductility and elasticity. The SLS process itself due to it's high temperature produce dried parts which gradually absorb humidity from air. This process can be accelerated by intentional soaking of built parts in water. Higher water temperature can enhance this process. One half of samples were dried / heated in furnace for 4 h in 110 °C. The other half was soaked in water for 4 h in 80 °C. All parts were tested within 5 h after treatment when they reached room temperature to prevent significant changes in part humidity by surrounding air water vapor content.

The key research process was the analysis of the torsional strength of the SLS samples. The tests were carried out with the use of a proprietary design of a test stand equipped with an advanced measuring system for determining the torque and torsion angle, as well as a precise adjustable drive system. The results were recorded and processed in real time using dedicated software.

The last stage of the research was the analysis of the fractures of the samples. For the fractures of the samples obtained after the static torsion test, surface morphology tests were carried out at ten times magnification using the KERN OZL-466 stereoscopic microscope.

RESULTS AND DISCUSSION

Dimensional and shape verification of test samples.

Dimensional and shape accuracy of parts working under torque load, including primarily machine shafts, hubs, couplings, is a key parameter that directly determines the possibility of using parts in a given area. It is therefore necessary to analyze the accuracy of model mapping in the incremental process, especially due to the individual conditions of each process – processing of numerical data, printout parameters, and above all, setting the model in the working space of the apparatus.

The geometry obtained after the printing process was compared with the geometry of the CAD model. Only the cylindrical area of the sample was selected for detailed examination. Tied ends with the mounting system in the measuring stadion – sample holders – omitted. The adjustment of the cylinder to the scan mesh was performed using the Best-fit Gauss 3 sigma method. The following parameters were obtained:

- roundness tolerances – two concentric circles limit the tolerance zone. The tolerance value defines the distance between the circles,
- cylindricity deviation – two coaxial cylinders limit the tolerance zone. The tolerance value defines the distance between the cylinders,
- concentricity deviation of the nominal cylinder constituting the CAD cylinder and the cylinder matched to the scan grid in accordance with the ISO 1101 standard – the function checks whether the center points or the center axes lie within a defined tolerance zone. The tolerance zone is circular. A cylinder limits the circular tolerance zone. The tolerance value defines the diameter of the cylinder,
- the deviation of the total runout relative to the axis of the sample's nominal cylinder. Measurement of the actual diameter within the ±0.2 deviation range.

In addition, it was possible to graphically display the best-fit layout of the CAD model and the sample scan grid.

The graphical comparison shows that technological errors in the surface topology are visible in all samples. They are manifested by visible limits of layering, especially for samples produced horizontally and at 45°. In addition, it can be stated, which coincides with the accepted standards, that the lowest axial deviations were obtained by samples manufactured at an angle of 45°. For samples produced horizontally, errors due to the ovalization of the samples play a major role. The lowest deviation of ovalization was obtained for samples produced vertically.

The results of the dimensional and shape verification of the test samples are shown in Figures 3–5 and in the summary Table 2.

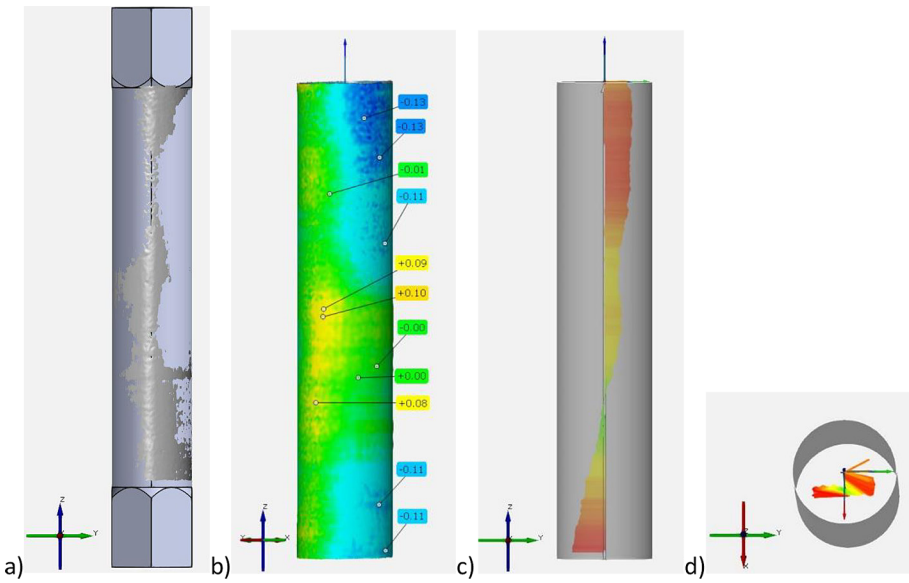

Figure 3. Graphical representation of the comparison for 3D printing for vertical manufacturing: a) best-fit representation, b) graphical representation of the deviation for a cylindrical part, c) deviation of the concentricity – axial view, d) deviation of the concentricity – radial view

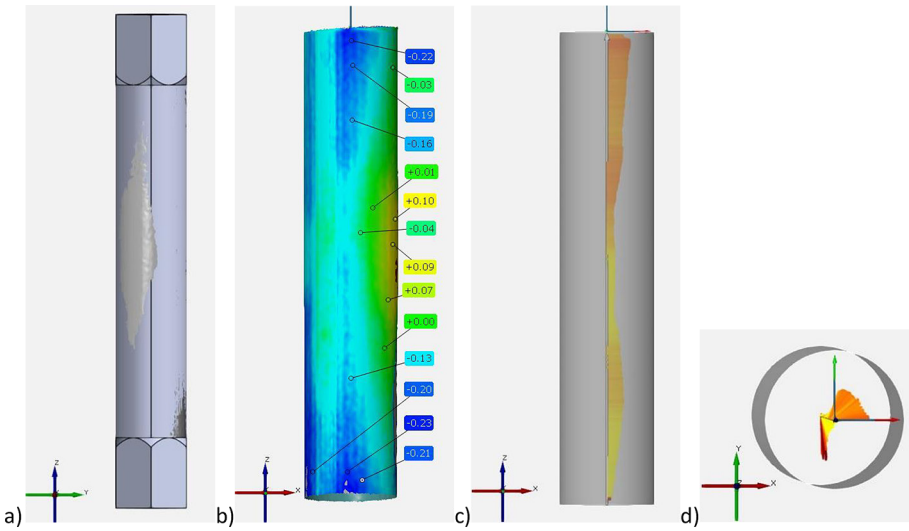

Figure 4. Graphical representation of the comparison for 3D printing for horizontal manufacturing: a) best-fit representation, b) graphical representation of the deviation for a cylindrical part, c) deviation of the concentricity – axial view, d) deviation of the concentricity – radial view

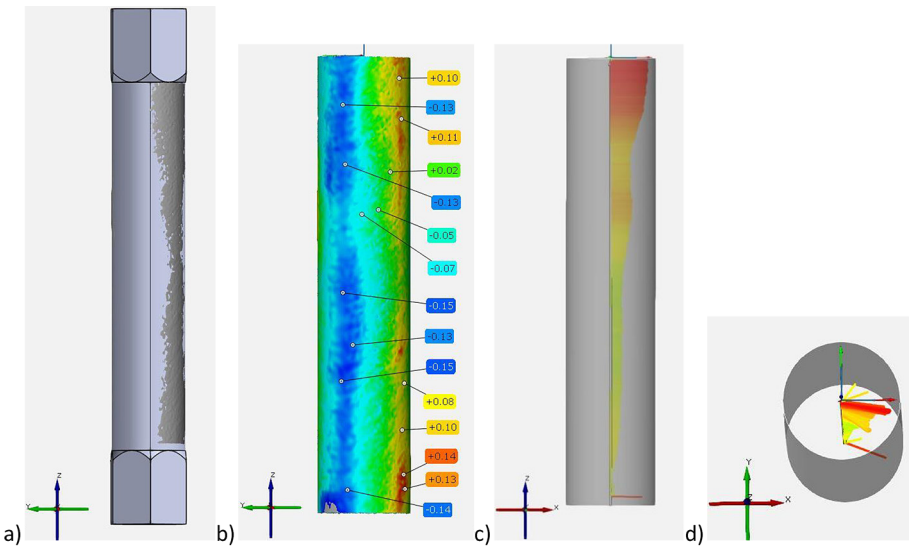

Figure 5. Graphical representation of the comparison for 3D printing for 45° manufacturing: a) best-fit representation, b) graphical representation of the deviation for a cylindrical part, c) deviation of the concentricity – axial view, d) deviation of the concentricity – radial view

Torsional strength analysis

Produced samples were functionally tested on mentioned torsional testbench. The results of the static torsion test of samples made of PA2200 material subjected to final treatment by soaking in water and heating in an oven are presented in tables 3 and 4. Based on the obtained results, mean values and standard deviation were calculated and coefficient of variation. The courses of the torque curves as a function of the torsion angle are shown in Figures 6–11.

On the basis of the obtained courses of torsion curves, it can be concluded that all samples made of PA2200 material using the SLS technique have the characteristics of elastic-plastic bodies. The plastic properties of the material are confirmed by a wide range of plasticity in the range of the average value of the torsion angle from 365 to 1034°. By analyzing the course of the torsion curve, a deformation characteristic of materials without a clear yield strength can be observed, therefore the stress causing the conventionally accepted relative deformation in the material is defined as the

Table 2. The results of the dimensional and shape verification of the test samples

Sample No.	Orientation relative to the working platform	Nominal diameter in CAD	Determined diameter of the SLS sample	Cylindricity deviation	Circularity deviation	Concentricity with CAD nominal shaft	Total run out relative to the nominal line – CAD, the axis of the model
1	vertically	20.00	19.87	0.26	0.17	0.20	0.29
2		20.00	19.92	0.32	0.26	0.37	0.34
3		20.00	19.95	0.29	0.18	0.24	0.36
4		20.00	19.88	0.28	0.16	0.24	0.29
1	horizontally	20.00	19.83	0.55	0.46	0.45	0.68
2		20.00	19.81	0.50	0.40	0.24	0.57
3		20.00	19.83	0.44	0.30	0.31	0.49
4		20.00	19.80	0.47	0.37	0.47	0.67
1	45°	20.00	19.93	0.38	0.29	0.14	0.42
2		20.00	19.92	0.45	0.34	0.15	0.51
3		20.00	19.96	0.44	0.40	0.28	0.51
4		20.00	19.91	0.34	0.31	0.22	0.37

Table 3. Static torsion test results of water-soaked samples produced in three orientations

Sample print orientation No.	Horizontally		45°		Vertically	
	Torsional torque [Nm]	Torsion angle [°]	Torsional torque [Nm]	Torsion angle [°]	Torsional torque [Nm]	Torsion angle [°]
Sample 1	65.3	896.3	62.3	825.3	63.5	328.6
Sample 2	65.8	880.9	63.0	660.2	64.9	388.2
Sample 3	66.0	959.2	63.2	723.5	64.4	378.7
Sample 4	66.1	854.8	61.7	551.7	63.2	364.8
Average	65.8	897.8	62.6	690.2	64.0	365.1
Deviation	0.3	38.4	0.6	99.3	0.7	22.6
Coefficient of variation [%]	0.5	4.3	0.9	14.4	1.1	6.2

conventional yield strength. After exceeding the conventional yield strength, permanent plastic deformation occurs (irreversible displacement of the layers), which is referred to as material flow. In all cases, after exceeding the yield strength, the plasticizing stresses (strengthening of the material) increase.

Figures 12 and 13 show a summary of the average torsional torque and torsional angle for each tested variant.

Analyzing the results obtained in the static torsion test, it can be seen that the strength of the samples produced by the SLS technology mainly depends on the type of post-processing

Table 4. Static torsion test results of furnace-heated samples (dried) produced in three orientations

Sample print orientation No.	Horizontally		45°		Vertically	
	Torsional torque [Nm]	Torsion angle [°]	Torsional torque [Nm]	Torsion angle [°]	Torsional torque [Nm]	Torsion angle [°]
Sample 1	71.4	944.0	70.8	816.5	71.3	705.1
Sample 2	71.3	965.5	71.2	813.5	71.5	704.8
Sample 3	71.4	1204.9	71.2	811.4	71.1	691.4
Sample 4	71.7	1022.3	71.3	805.9	70.7	757.1
Average	71.5	1034.2	71.1	811.8	71.2	714.6
Deviation	0.2	102.6	0.2	3.9	0.3	25.2
Coefficient of variation [%]	0.2	9.9	0.3	0.5	0.4	3.5

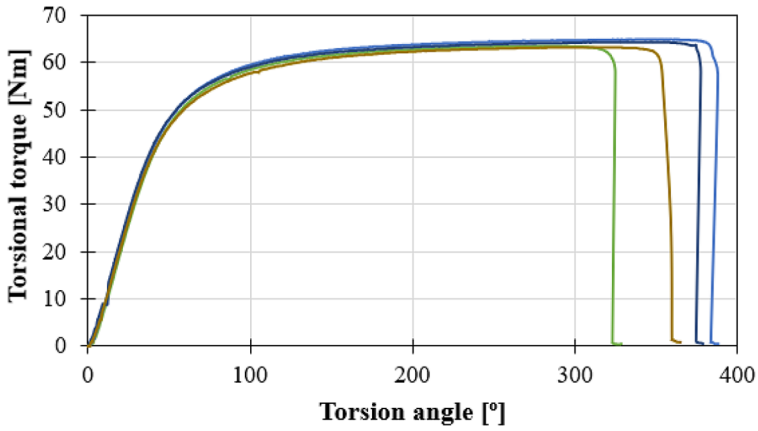

Figure 6. Graph of the torsion moment as a function of the torsion angle of water-soaked samples set vertically

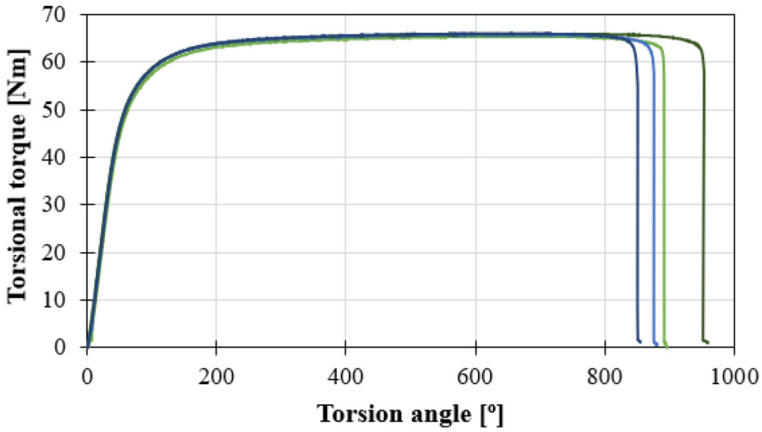

Figure 7. Graph of the torsion moment as a function of the torsion angle of water-soaked samples set horizontally

treatment used. The summary of the maximum values of the transmitted torque, presented in Figures 12 and 13, depending on the applied final treatment of the test models and their orientation relative to the working platform of the device, shows that the samples that were furnace-heated samples had higher torsional strength. With regard to the average values of the torque in the case of furnace-heated samples, the increase in value was about 14%, compared to water-soaked samples. For the SLS technology, the anisotropy is up to about 10 %, while in

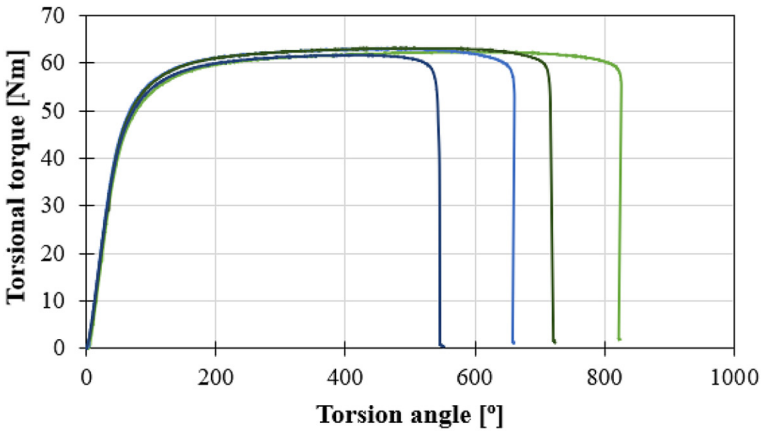

Figure 8. Graph of the torsion moment as a function of the torsion angle of water-soaked samples set at an angle of 45°

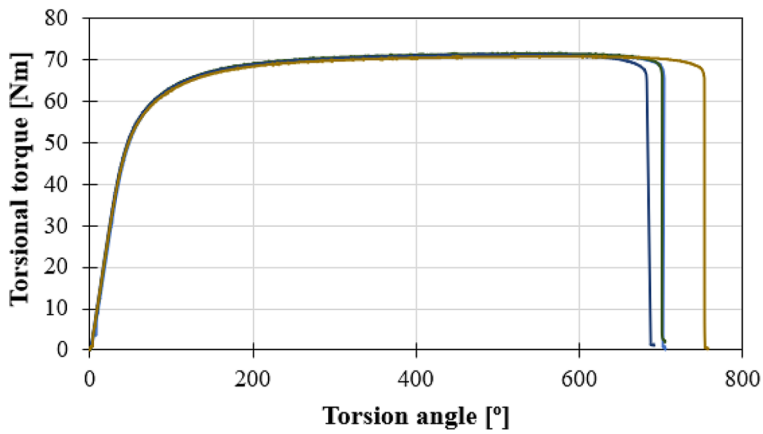

Figure 9. Graph of the torsion moment as a function of the torsion angle of furnace-heated samples set vertically

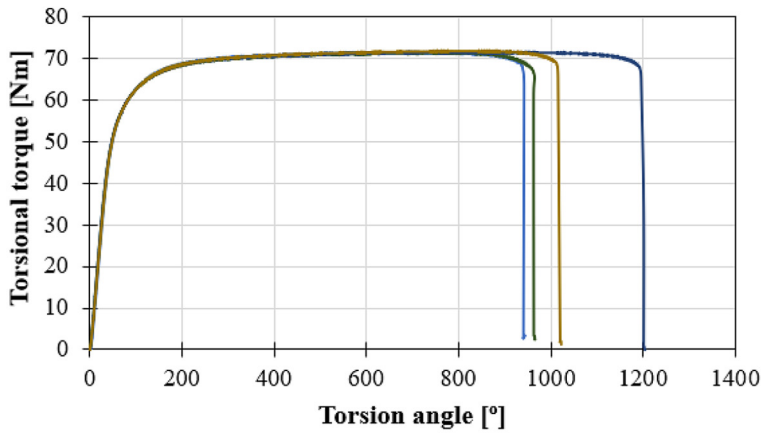

Figure 10. Graph of the torsion moment as a function of the torsion angle of furnace-heated samples set horizontally

the case of the obtained test results, for water-soaked samples, the anisotropy was 5.2 %, and for furnace-heated samples, 0.4%. It should also be noted that the value of the maximum torsion angle (regardless on the type of post-processing) depends on the arrangement of the model in the working space of the manufacturing equipment. The samples arranged vertically in relation to the printer's working platform had the lowest values of the maximum twist angle.

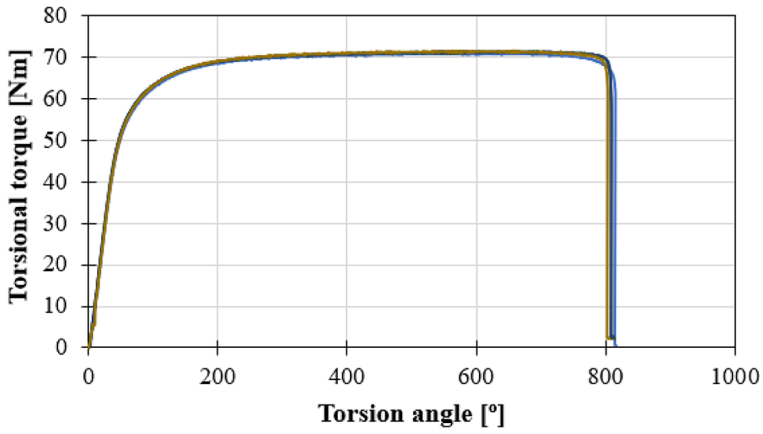

Figure 11. Graph of the torsion moment as a function of the torsion angle furnace-heated samples set at an angle of 45°

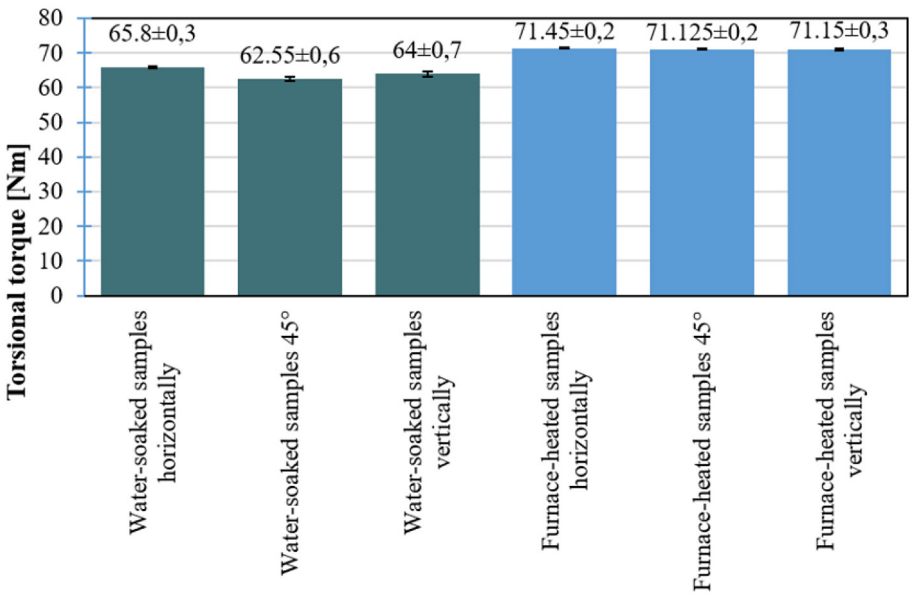

Figure 12. Comparisons of the average values of the torsional torque

Samples fractures analysis.

For the fractures of the samples obtained after the static torsion test, surface morphology tests were carried out at ten times magnification using the KERN OZL-466 stereoscopic microscope. The selected result of the analysis of the SLS sample fracture – a microscopic image – is shown in Figure 14.

Based on the results of the observation of fractures of samples obtained from powdered PA2200 polyamide, it can be unequivocally stated that in all cases the fracture obtained on a macroscopic scale is characterized by a silky surface with low roughness. This is directly related to the intense plastic deformation and the accumulation of deformation energy in the material. The obtained ductile (plastic) fracture occurs in the material under the influence of stresses greater than the yield strength. This process is associated with a large plastic deformation, so it requires significant energy expenditure for crack propagation. The course of ductile cracking can be stopped at any time as a result of reducing the stress below the material's yield strength. Hence, ductile cracking is not as dangerous as brittle cracking and it does not happen too often in the operation of machines and various types of equipment.

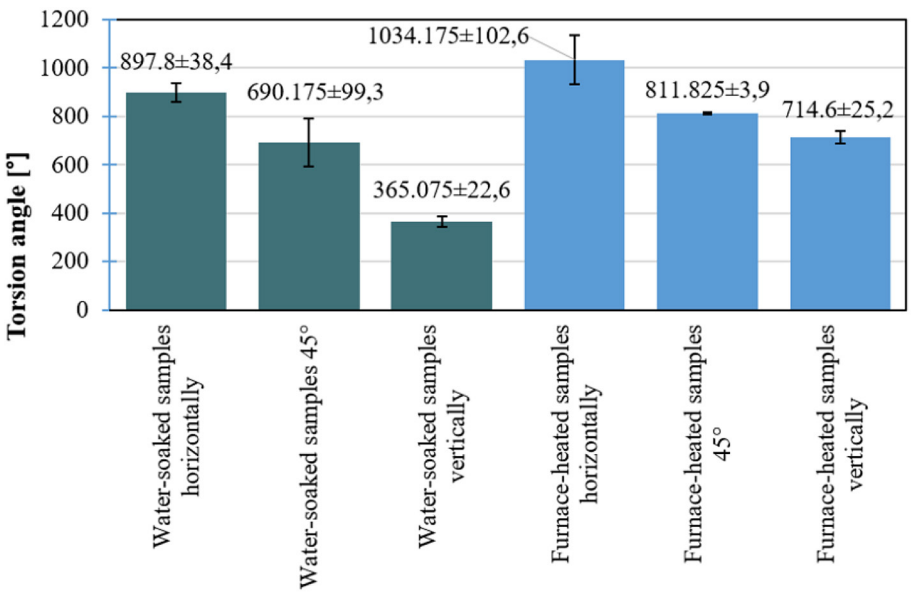

Figure 13. Comparisons of the average values of the torsion angle

Figure 14. Fracture of water-soaked sample in vertical orientation

CONLUSIONS

The research process of analyzing the torsional strength of standard samples with a circular cross-section, incrementally produced by the SLS technique from polyamide PA2200 significantly supplemented the existing knowledge in terms of strength parameters, which in the present case, i.e. torsional strength, are currently not published by the manufacturers of model materials. The wide range of applications of additively manufactured parts also applies to components working under complex loads, including torque, such as machine shafts, hubs, couplings, etc. Therefore, the conducted research is of key importance in the process of designing and implementing the indicated machine parts for production.

The initial dimensional and shape verification showed that technological errors in the surface topology are visible in all samples. They are manifested by visible limits of layering, especially for samples produced horizontally and at 45°. In addition, it can be stated, which coincides with the accepted standards, that the lowest axial deviations were obtained by samples manufactured at an angle of 45°. For samples produced horizontally, errors due to the ovalization of the samples play a major role. The lowest deviation of ovalization was obtained for samples produced vertically.

The analysis of the test results in the static torsion test allows to conclude that the strength of the samples produced by the SLS technology depends mainly on the type of post-processing treatment used. Higher torsional strength was determined for the furnace-heated samples. In addition, it was found that the value of the maximum torsion angle (regardless of the type of post-processing) depends on the arrangement of the model in the working space of the manufacturing equipment. The samples arranged vertically in relation to the printer's working platform had the lowest values of the maximum torsion angle.

The fracture analysis of the samples carried out at the last stage of the research showed that in all cases the fracture obtained on a macroscopic scale is characterized by a silky surface with low roughness. This is directly related to the intense plastic deformation and the accumulation of deformation energy in the material. The obtained fracture is ductile (plastic), it occurs in the material under the influence of stresses greater than the yield strength.

The results of the torsional strength analysis and the dimensional and shape verification of models made of PA2200 material shaped with the SLS technique, determined in the research process, can be used to define the potential area of application of the material in question that is – polymer powder and sintering technique for the production of parts subjected to complex dynamical loads.

The area of planned future research will be the analysis of the torsional strength of other commonly used polymeric materials processed with AM techniques, for which the parameters in question have not been published. In addition, comprehensive strength tests of new composite materials produced for the needs of AM will be undertaken.

Acknowledgments

The publication was financed from the funds of the Polish Ministry of Education and Science as part of the program,,Social Responsibility of Science / Excellent Science", support for Scientific Conferences,,Synergy of Science and Industry", Challenges of the 21st Century, Science – Industry – Business.

REFERENCES

1. Wohlers Report, 3D Printing and Additive Manufacturing State of the Industry, Annual Worldwide Progress Report, 2018.
2. Orth A., Sampson K.L., Zhang Y., Ting K., Aranguren van Egmond D., Laqua K., Lacelle T., Webber D., Fatehi D., Boisvert J., Paquet C. On-the-fly 3D metrology of volumetric additive manufacturing. Additive Manufacturing 2022; 56: 2022.
3. Górski F., Wichniarek R., Kuczko W., Żukowska M., Szuszek E., Rapid Manufacturing of Individualized Prosthetic Sockets. Advances in Science and Technology Research Journal 2020; 14(1): 42–49.
4. Manjaiah M., Raghavendra K., Balashanmugam N., Paulo Davim J. Additive Manufacturing: A Tool for Industrial Revolution 4.0, Elsevier Science 2021.
5. Wi K., Suresh V., Wang K., Li B., Qin H. Quantifying quality of 3D printed clay objects using a 3D structured light scanning system. Additive Manufacturing 2020; 32.
6. Dziubek T., Budzik G., Kawalec A., Dębski M., Turek P., Oleksy M., Paszkiewicz A., Poliński P., Kochmański Ł., Kiełbicki M., Józwik J., Kuric I., Cebulski J. Strength of threaded connections additively produced from polymeric materials. POLIMERY 2022; 67(6): 261–270.
7. Guerra M.G., Volpone C., Galantucci L.M., Percoco G., Photogrammetric measurements of 3D printed microfluidic devices. Additive Manufacturing 2018; 21: 53–62.
8. Vora H.D., Sanyal S. A comprehensive review: metrology in additive manufacturing and 3D printing technology. Progress in Additive Manufacturing 2020; 5: 319–353.
9. Gao X., Kuang X., Li J., Qi S., Su Y., Wang D., Fused filament fabrication of polymer materials: A review of interlayer Bond. Additive Manufacturing 2021; 37.
10. Badiru A.B., Valencia V.V., Liu D. Additive Manufacturing Handbook. Product Development for the Defense Industry, CRC Press, 2020.
11. Bell D., Siegmund T. 3D-printed polymers exhibit a strength size effect. Additive Manufacturing 2018; 21: 658–665.
12. Królczyk G., Kacalak W., Wieczorowski M. 3D Parametric and Nonparametric Description of Surface Topography in Manufacturing Processes. Materials 2021; 14(8).
13. Birosz, M.T., Ledenyák, D., Andó, M. Effect of FDM infill patterns on mechanical properties. Polymer Testing 2022; 113.
14. Koteras R., Wieczorowski M., Znaniecki P., Swojak N. Measurement strategy as a determinant of the measurement uncertainty of an optical scanner. Archives of Mechanical Technology and Materials 2019; 39(1): 26–31.
15. Wieczorowski M., Yago I.P., Pereira D.A., Gapiński B., Budzik G., Diering M. Comparison of Measurements Realized on Computed Tomograph and Optical Scanners for Elements Manufactured by Wire Arc Additive Manufacturing, Advances in Manufacturing III, Volume 4 – Measurement and Control Systems: Research and Technology Innovations, Industry 4.0, Switzerland, Springer 2022; 127–141.
16. Bernaczek J., Dębski M., Gontarz M., Kiełbicki M., Magniszewski M., Przeszłowski Ł. Influence of torsion on the structure of machine elements made of polymeric materials by 3D printing. POLIMERY 2021; 66(5): 298–304.
17. Budzik G., Magniszewski M., Oleksy M., Oliwa R., Bernaczek J., Torsional strengh testing of machine elements manufacture by incremental technology from polymeric materials. POLIMERY 2018; 63(11–12): 830–832.
18. Fontana L., Minetola P., Iuliano L., Rifuggiato S., Khandpur M.S., Stiuso V. An investigation of the influence of 3D printing parameters on the tensile strength of PLA material. Materials Today, Proceeding 2022; 57(2): 657–663.
19. Oleksy M., Oliwa R., Bulanda K., Budzik G., Przeszłowski Ł., Magniszewski M., Paszkiewicz A., Torsional strength test of spline connections made of polimer materials. POLIMERY 2021; 66(1): 52–55.
20. Cobian L., Rueda-Ruiz M., Fernandez-Blazquez J.P., Martinez V., Galvez F., Karayagiz F., Lück T., Segurado J., Monclus M.A. Micromechanical characterization of the material response In a PA12-SLS fabricated lattice structure and its correlation with bulk behaviour. PolymerTesting 2022; 110.
21. Zubrzycki J., Estrada Q., Staniszewski M., Marchewka M. Influence of 3D Printing Parameters by FDM Method on the Mechanical Properties of Manufactred Parts. Advances in Science and Technology Research Journal 2022; 16(5): 52–63.

22. EOS GmbH – Electro Optical Systems, Product Information datasheet – Finepolyamide PA 2200 for EOSINT P (https://3dformtech.fi/wp-content/uploads/2019/11/Material-Data-PA2200.pdf).
23. Bourell D.L., Sintering in Laser Sintering, JOM 2016; 68: 885–889.
24. Stoia D.I., Linul E., Marsavina L. Influence of Manufacturing Parameters on Mechanical Properties of Porous Materials by Selective Laser Sintering, Materials (Basel) 2019; 12(6).
25. Thiede S., Wiese M., Herrmann Ch. Upscaling strategies for polymer additive manufacturing: anassessment from economic and environmental perspective for SLS, MJF and DLP. Procedia CIRP 2021; 104: 653–658.
26. Schmid M., Amado A., Wegener K. Materials perspective of polymers for additive manufacturing with selective laser sintering. Journal of Materials Research 2014; 29(17): 1824–1832.
27. Barchiesi E., Ganzosch G., Liebold C., Placidi L., Grygoruk R., Müller W.H. Out-of-plane buckling of pantographic fabrics in displacement-controlled shear tests: experimental results and model validation. Continuum Mechanics and Thermodynamics 2019; 31: 33–45.
28. Turco E., Dell'Isola F., Luigi Rizzi N., Grygoruk R., Müller W.H., Liebold C. Fiber rupture in sheared planar pantographic sheets: Numerical and experimental evidence. Mechanics Research Communications 2016; 76: 86–90.
29. Razaviye M.K., Tafti R.A., Khajehmohammadi M. Aninvestigation on mechanical properties of PA12 parts produced by a SLS 3D printer: An experimental spproach. CIRP Journal of Manufacturing Science and Technology 2022; 38: 760–768.
30. Golaszewski M., Grygoruk R., Giorgio I., Laudato M., Di Cosma F. Metamaterials with relative displacements in their microstructure: technological challenges in 3D printing, experiments and numerical predictions. Continuum Mechanicsand Thermodynamics 2019; 31: 1015–1034.
31. Rajesh J.J., Bijwe J., Venkataraman B. Effect of water absorption on erosive wear behaviour of polyamides. Journal of Materials Science 2002; 37: 5107–5113.